Phys. Status Solidi C 7, No. 3–4, 1033–1036 (2010) / DOI 10.1002/pssc.200982778

physica status solidi c
www.pss-c.com
current topics in solid state physics

2D simulations of interdigitated back contact heterojunction solar cells based on n-type crystalline silicon

D. Diouf[1,*], J.P. Kleider[1], T. Desrues[2], and P.J. Ribeyron[2]

[1] LGEP, CNRS UMR8507, SUPELEC, Univ Paris-Sud, UPMC Univ Paris 6, 11 rue Joliot-Curie, Plateau de Moulon, 91192 Gif-sur-Yvette Cedex, France
[2] INES-CEA Grenoble, 50 Avenue du Lac Léman, 73370 Le Bourget du Lac, France

Received 1 August 2009, revised 2 November 2009, accepted 7 November 2009
Published online 8 February 2010

PACS 73.40.Lq, 84.60.Bk, 84.60.Jt, 85.40.Ls

* Corresponding author e-mail: djicknoum.diouf@lgep.supelec.fr, Phone: +33-169-851-680, Fax: +33-169-418-318

The combination of amorphous silicon/crystalline silicon heterojunction (a-Si:H/c-Si) concept with interdigitated back contact leads to a very promising structure for high efficiency solar cell. In this work, we study the interdigitated back contact silicon heterojunction (IBC-SiHJ) structure by two-dimensional numerical simulations and we focus on IBC-SiHJ solar cells based on n-type c-Si. Assuming low surface recombination velocity (10 cm/s), we study the effect of the following parameters: bulk lifetime and doping concentration of c-Si, density of defects at the a-Si:H/c-Si interface. The influence of these parameters has been tested by generating the current-voltage (I-V) curves. Results indicate that with a high crystalline substrate quality and low recombining a-Si:H/c-Si interfaces efficiencies approaching 25% can be reached.

1 Introduction The solar cells based on amorphous silicon (a-Si:H)/ crystalline silicon (c-Si) heterojunction (SiHJ) with n-type c-Si as substrate have demonstrated their ability to reach high conversion efficiency (23%) [1]. The association of SiHJ technique with the interdigitated back contact concept can lead to a high efficient solar cell. Previous simulations of interdigitated back contact silicon heterojunction (IBC SiHJ) solar cells [2] based on p-type c-Si had shown the potential of this type of cell and pointed out several limiting factors for this type of cell: front surface passivation, quality of a-Si:H/c-Si interfaces, quality of contacts (series resistance, metal coverage and metal work function). Based on better experimental results and on theoretical approaches, the use of n-type c-Si instead of p-type c-Si is obvious [3, 4].We focus here on the IBC SiHJ solar cell based on n-type c-Si and study the influence of the bulk resistivity and the a-Si/c-Si heterointerfaces on the cell performance.

2 Structure and physical parameters The reference structure of the IBC-SiHJ solar cell used in our numerical simulations is presented in Fig. 1. The geometrical and material parameters of the simulated device were chosen in agreement with a realistic fabrication process [5].

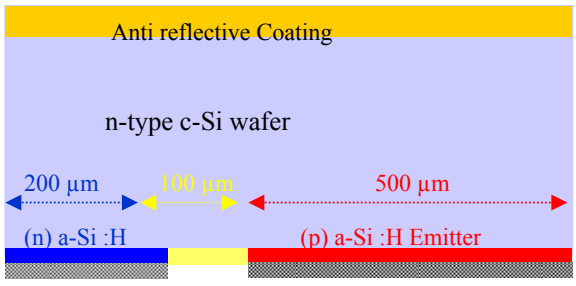

Figure 1 Device structure of IBC-SiHJ solar cell used in our simulations.

A 250 µm n-type polished crystalline silicon wafer is used as the substrate. We define two electrodes at the rear of the wafer: a p-type a-Si:H emitter and an n-type a-Si:H back surface field. The 100 µm wide region between the two doped layers (gap region) is modelled with an insulator

layer. BSF and emitter are totally covered with metal contacts. The pitch, defined as half of the distance between two electrode fingers of the same polarity, is set at 0.8 mm (see Fig. 1).

For a-Si:H layers, the distribution of the density of states (DOS) is a combination of two exponentially decaying band tail states (donor-like valence band tail and acceptor-like conduction band tail) and two Gaussian distributions of deep defect states (one donor-like, the other acceptor-like) [6] that were chosen in order to be compatible with the defect pool model (in particular regarding their position and amplitude as a function of Fermi level position) [7]. The DOS and doping concentrations were adjusted to set the Fermi level at room temperature at 0.32 eV below the conduction band edge in (n) a-Si:H (BSF) and at 0.3 eV above the valence band edge in (p)a-Si:H (emitter), values corresponding to experimental data of the activation energies of the dark conductivity in these layers.

Simulations were performed using the numerical device simulator ATLAS from Silvaco International [8]. The simulation is based on the resolution of the three governing semiconductor equations: Poisson's equation, electron and hole continuity equations. The Boltzmann statistics is used for carriers with the drift-diffusion model in ATLAS. Recombination of carriers through Auger and Shockley-Read-Hall (SRH) mechanisms were also modelled as a function of doping concentration. The lifetime associated to Shockley-Read-Hall recombination [9] is described by the expression:

$$\tau_{SRH} = \frac{\tau_{0,SRH}}{1 + \frac{N_{c-Si}}{N_{SRH}}}, \quad (1)$$

where $N_{c\text{-}Si}$ is the doping concentration of c-Si, and N_{SRH} is a constant with default value equal to 5×10^{16} cm^{-3}.

Assuming low injection conditions and that the dark values of np^2 and n^2p (n and p being the electron and hole concentrations, respectively) are negligible compared to their values under light, the lifetime corresponding to Auger recombination process is defined for n-type c-Si by:

$$\tau_{Aug} = \frac{1}{C_N N_{c-Si}^{\ 2}}, \quad (2)$$

where the Auger coefficient C_N is calculated according to Kerr-Cuevas parametrization [10]:

$$C_N = 1.9 \times 10^{-24} \times N_{c-Si}^{\ -0.35}. \quad (3)$$

The AM1.5G solar spectrum was used for the optical generation to simulate current-voltage, $I(V)$, curves under standard one-sun illumination conditions at an intensity of 100 mW/cm^2.

3 Simulations results From the simulated $I(V)$ curves we have evaluated the four main output parameters of the solar cell: open-circuit voltage, V_{OC}, short circuit current density, J_{SC}, efficiency, η, and fill factor, FF. We calculate $I(V)$ curves considering no reflection losses at the front surface that gives an indication of the best cell performance that could be obtained in textured wafers. The results shown here are obtained assuming good passivation of the front and back surfaces i.e. low surface recombination velocity of carriers (SRV=10 cm/s).

3.1 Impact of c-Si resistivity The influence of c-Si resistivity in the performance of heterojunction solar cells is still not very clear despite several studies [11-13]. The equations governing the dependence of bulk resistivity upon recombination are often simplified. In the following, we try to find out the influence of the different doping-related parameters in solar cell performances. Assuming good passivation at the front and rear surfaces and low recombining a-Si:H/c-Si interfaces, the bulk lifetime is determined by SRH and Auger recombination process and these processes depend on the doping concentration. The c-Si resistivity is related to the doping concentration by:

$$\rho = \frac{1}{e\mu_n N_{c-Si}}, \quad (4)$$

where e is the unit charge and μ_n the electron mobility that was taken dependent on the doping concentration [14]. In Fig. 2, the bulk lifetime defined as:

$$\frac{1}{\tau_{bulk}} = \frac{1}{\tau_{SRH}} + \frac{1}{\tau_{Aug}}, \quad (5)$$

is calculated taking account of both SRH and Auger contributions (surface recombination is neglected) as function of doping concentration.

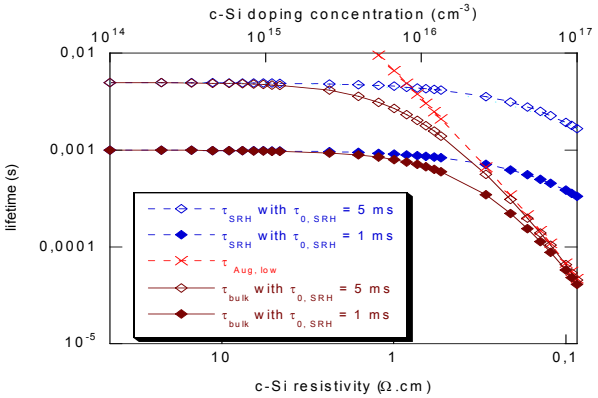

Figure 2 Variations of the bulk lifetime as a function of the c-Si doping concentration (upper x axis) and of bulk resistivity (lower x axis).

We can observe that Auger recombination becomes dominant at high doping concentration (low bulk resistivity).

The impact of c-Si resistivity on the IBC SiHJ solar cell outputs is shown in Figs. 3, 4 and 5.

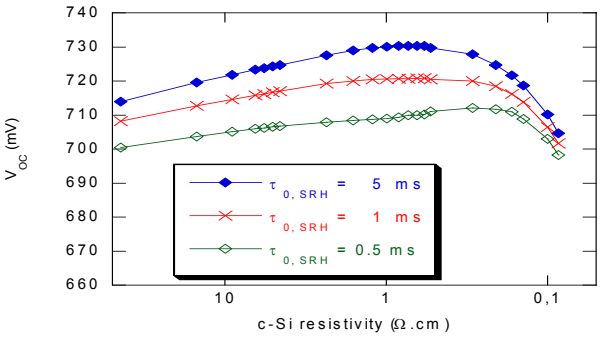

Figure 3 Variations of IBC-SiHJ solar cell open-circuit voltage as a function of bulk resistivity with different substrate qualities. No interface defects and *SRV*=10 cm/s at front and back surfaces.

As seen in Fig. 3, V_{OC} first increases when the c-Si resistivity decreases, up to a doping concentration of the order of $N_{c\text{-}Si}$=5×10^{16} cm^{-3} where Auger recombination is so strong that it makes V_{OC} decrease.

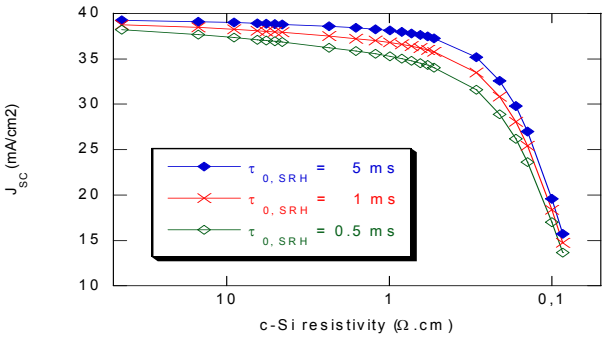

Figure 4 Variations of IBC-SiHJ solar cell short circuit current as a function of bulk resistivity with different substrate qualities. No interfaces defects and *SRV*=10 cm/s at front and back surfaces.

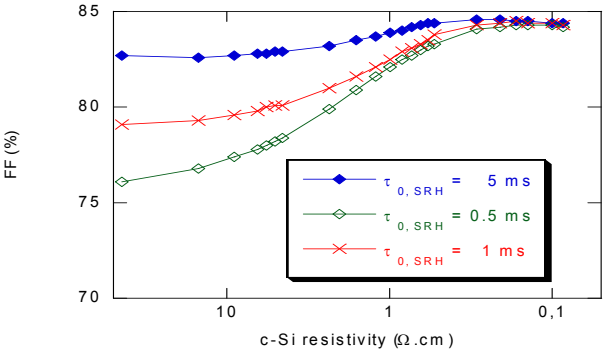

Figure 5 Variations of the fill factor of IBC-SiHJ solar cells as a function of bulk resistivity with different substrate qualities. No interfaces defects and *SRV* = 10 cm/s at front and back surfaces.

The short circuit current first only slowly decreases with decreasing resistivity (down to 3 Ω.cm) due to lower lifetime of carriers, and the decrease is more pronounced when Auger recombination plays a major role, as shown in Fig. 4. In Fig. 5, the fill factor of IBC SiHJ solar cell is shown to increase with decreasing resistivity. This can be explained by a lower potential drop with lower substrate resistivity. Note that the high value obtained for the fill factor is explained by the low contact resistance value (0.01 Ω. cm^2) used in our simulations.

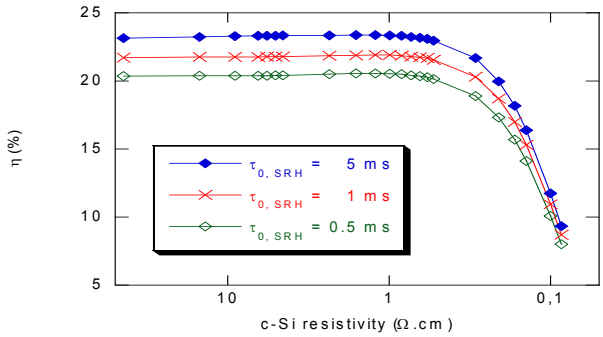

Figure 6 Variations of the efficiency of IBC-SiHJ solar cells as a function of bulk resistivity with different substrate qualities. No interfaces defects and *SRV*=10 cm/s at front and back surfaces.

The different variations of the IBC SiHJ solar cell outputs (V_{OC}, J_{SC} and *FF*) induce the existence of an optimum for bulk resistivity, as can be seen in Fig. 6. The maximum in efficiency is very flat, so bulk resistivity can be chosen in a wide interval: $0.6 < \rho < 30$ Ω.cm is adapted to yield more than 99% of maximum performance. Note that the optimum also depends on the rear side geometry and the value of the pitch, but also on the front surface structure [15]. Further simulations (not shown here) proved that by optimization of the pitch and of the reflection at the back contacts efficiencies of up to 25% can be reached with IBC SiHJ solar cells based on n-type c-Si.

3.2 Impact of a-Si:H/c-Si hetero-interfaces In this section, the influence of a-Si:H/c-Si interface in the performances of IBC SiHJ solar cell is studied. With our simulations, we determine the impact of each hetero-interface (a-Si:H(n)/c-Si(n) or a-Si:H(p)/c-Si(n)) in the solar cell performances.

To take account of interface recombination, we introduced a defective c-Si layer at the interface between a-Si:H and c-Si with a thickness d_{int}=1nm. The defect distribution in this interface layer was assumed to be a Gaussian of donor-like defects located at 0.56 eV above the valence band maximum, with a characteristic σ parameter of 0.14 eV. In the following N_{SS} (in cm^{-2}) will denote the interface defect density, which is determined as the product $d_{int}\times N_{it}$ where N_{it} (in cm^{-3}) is the total defect density in this layer, which is the integral over the band gap of the Gaussian DOS, g_{it} (in cm^{-3}eV^{-1}). Capture cross sections for both types of carriers were taken equal to 10^{-15} cm^2 for these interface states. The defect states increase surface recombination at these hetero-interfaces and thus decrease the solar cell performance. The recombination due to the defect states depends on their density and their capture cross-sections of carriers. The capture cross section of carriers is fixed at $\sigma_n = \sigma_p =$

10^{-15} cm^2 and their density is varied. We introduced defect states at each hetero-interface separately and also at both hetero-interfaces simultaneously.

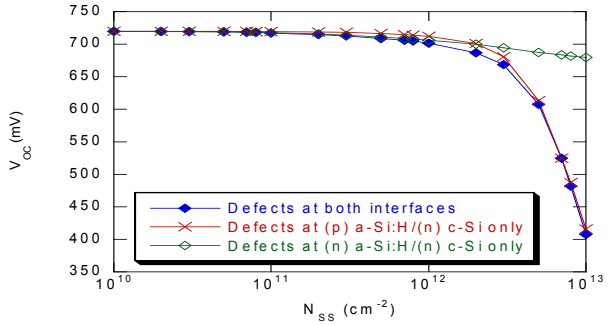

Figure 7 Variations of IBC-SiHJ solar cells open-circuit voltage as a function of interface defect density. Values of bulk c-Si parameters are $N_{c\text{-}Si} = 3\times10^{15}$ cm^{-3} and $\tau_{0,SRH} = 1$ ms.

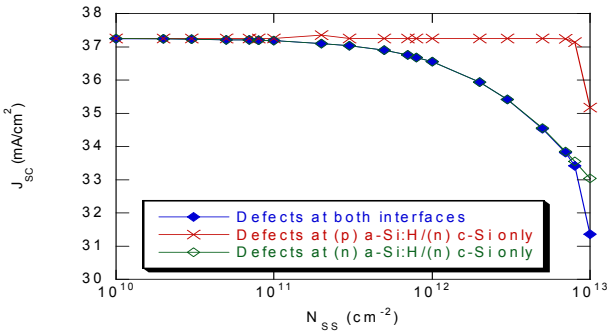

Figure 8 Variations of IBC-SiHJ solar cells short circuit current as a function of interface defect density. Values of bulk c-Si parameters are $N_{c\text{-}Si} = 3\times10^{15}$ cm^{-3} and $\tau_{0,SRH} = 1$ ms.

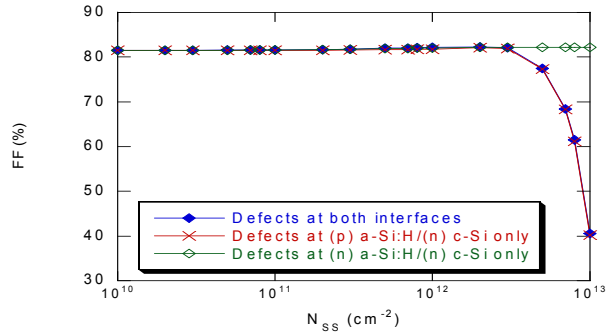

Figure 9 Variations of IBC-SiHJ solar cell fill factor as a function of interface defect density. Values of bulk c-Si parameters are $N_{c\text{-}Si} = 3\times10^{15}$ cm^{-3} and $\tau_{0,SRH} = 1$ ms.

The evolution of V_{OC} as a function of interface defect density is presented in Fig. 7. V_{OC} is affected whatever the location of the defects (at either emitter or BSF). The short circuit current is affected by defect states at the BSF, (n)a-Si:H/(n)c-Si hetero-interface, as seen in Fig. 8, while the fill factor is affected by high defect states at the emitter (p)a-Si:H/(n)c-Si hetero-interface, as depicted in Fig. 9.
IBC-SiHJ solar cell is very sensitive to surface defects density and capture cross section of carriers. Their performances are affected by interface defect density up to 10^{12} cm^{-2} for $\sigma = 10^{-15}$ cm^2. So special care has to be taken to have good passivation at the a-Si:H/c-Si hetero-interface.

4 Conclusion 2D numerical simulations were performed in order to study the IBC SiHJ solar cell based on n-type crystalline silicon. With low surface recombination and low recombining a-Si:H/c-Si hetero-interfaces, the c-Si resistivity can be chosen in a wide interval, between 0.6 and 30 Ω.cm for optimal cell performance. Our simulations also pointed out the impact of defect states at each a-Si:H/c-Si hetero-interface (emitter or BSF) on the cell outputs (short circuit current, open-circuit voltage and fill factor). They demonstrate the high potential of the IBC SiHJ solar cell for high efficiency. Efficiencies of 23.5 % are obtained for reasonable parameters of the c-Si and a-Si;:H layers. After further optimization of rear side geometry, efficiency can approach 25 %.

Acknowledgements This work was partly supported by Agence Nationale de la Recherche (ANR) in the framework of the QCPASSI project, and by European Community's Seventh Framework Programme (FP7/2007-2013) under grant agreement no. 211821 (HETSI project).

References

[1] Sanyo, Japan, press release (2009).
[2] D. Diouf, J. P. Kleider, T. Desrues, and P.-J. Ribeyron, Mater. Sci. Eng. B **159/160**, 291 (2009).
[3] J. E. Cotter, J. H. Guo, P. J. Cousins, M. D. Abbott, F. W. Chen, and K. C. Fisher, IEEE Trans. Electron. Dev. **53**, 1893 (2006).
[4] M. Yamaguchi, Y. Ohshita, K. Arafune, H. Sai, and M. Tachibana, Solar Energy **80**, 104 (2006).
[5] T. Desrues P-J. Ribeyron, A. Vandeneynde, A.-S. Ozanne, F. Souche, Y. Veschetti, A. Bettinelli, P. Roca i Cabarrocas, M. Labrune, D. Diouf, J.-P. Kleider, and M. Lemiti, in: Proceedings 23rd EPVSEC, Valence, Spain, 2008, pp. 1673-1676.
[6] A. S. Gudovskikh, S. Ibrahim, J.-P. Kleider, J. Damon-Lacoste, P. Roca i Cabarrocas, Y. Veschetti, and P.-J. Ribeyron, Thin Solid Films **515**, 7481 (2007).
[7] M.J. Powell and S. Deane, Phys. Rev. B **48**, 10815 (1993)
[8] User's manual for ATLAS from Silvaco International, version 5. 12.1.
[9] J. G. Fossum and D.S. Lee, Solid State Electron. **25**, 741 (1982).
[10] M. J. Kerr and A. Cuevas, J. Appl. Phys. **91**, 2473 (2002).
[11] C. Jacoboni, C. Canali, G. Ottaviani, and A. A. Quaranta, Solid State Electron. **20**, 77 (1977).
[12] J. A. Del Alamo, and R. M. Swanson, Solid State Electron. **30**, 1127 (1987).
[13] M. J. Kerr, PhD Thesis, June 2002.
[14] G. Masetti, M. Severi and S. Solmi, IEEE Trans. Electron. Dev. **30**, 764 (1983).
[15] M. Hermle, F. Glanek, O. Schultz, and S. Glunz, J. Appl. Phys. 103, 054507 (2008).

